



Contents lists available at ScienceDirect

Journal of Cleaner Production

journal homepage: www.elsevier.com/locate/jclepro

Increasing the productivity of the wire-cut electrical discharge machine associated with sustainable production

Ibrahim Maher ^{a, b}, Ahmed A.D. Sarhan ^{a, c, *}, Mohsen Marani Barzani ^a, M. Hamdi ^a

^a Centre of Advanced Manufacturing and Material Processing, Department of Mechanical Engineering, Faculty of Engineering, University of Malaya, 50603 Kuala Lumpur, Malaysia

^b Department of Mechanical Engineering, Faculty of Engineering, Kafrelsheikh University, Kafrelsheikh 33516, Egypt

^c Department of Mechanical Engineering, Faculty of Engineering, Assiut University, Assiut 71516, Egypt

ARTICLE INFO

Article history:

Received 16 October 2014

Received in revised form

10 June 2015

Accepted 10 June 2015

Available online xxx

Keywords:

Sustainable production

Energy consumption

Wire-cut EDM

ANFIS

Taguchi

ABSTRACT

Wire-cut electric discharge machining is a nontraditional technique by which the required profile is acquired using sparks energy. Concerning wire-cut electric discharge machining, high cutting rates and precision machining is necessary to improve productivity and achieve high quality of machined workpieces. In this research work, an experimental investigation was introduced to achieve higher productivity of the wire electrode associated with sustainable production in terms of product quality and less heat-affected zone. For this purpose, the effects of machining parameters including peak current, pulse on time and wire preloading were investigated using adaptive neuro-fuzzy inference system along with the Taguchi method. From this study, the optimal setting of machining parameters to achieve higher productivity and sustainability was identified. Moreover, Neuro-fuzzy modeling was successfully used to build an empirical model for the selection of machining parameters to achieve higher productivity at highest possible surface quality and minimum cost for sustainable production.

© 2015 Elsevier Ltd. All rights reserved.

1. Introduction

Wire-cut electric discharge machining (Wire-cut EDM) is an advanced machining process for machining complicated shapes of hard conductive materials (Sommer and Sommer, 2013). Wire-cut EDM is usually used when low residual stresses are required, because it does not entail high cutting forces for material removal. Wire-cut EDM can machine any electrically conductive materials regardless of the hardness, from common materials such as copper, aluminum, tool steel, and graphite, to unusual modern alloys including wafer silicon, Inconel, titanium, carbide, polycrystalline diamond compacts. Besides, Wire-cut EDM is also used to machine modern composite materials such as conductive ceramics (Ho et al., 2004; Maher et al., 2015c). In Wire-cut EDM, the workpiece is machined with a series of electrical sparks that are produced between the workpiece and the wire electrode. The wire electrode discharges high frequency pulses of alternating or direct current to

the workpiece through a very small spark gap with a nonconductive dielectric fluid. Many sparks can be easily seen instantaneously at the cutting zone because sparks happen more than one hundred thousand times per second (El-Hofy, 2005). Cutting rate and surface quality are usually used to optimize the material removal rate (productivity) during the period of spark discharge. The productivity in Wire-cut EDM associated with sustainable production depend on a large number of machining parameters, as shown in Fig. 1, like electrical spark (discharge current, pulse width, etc.), wire electrode (shape, tension, material and speed), workpiece (high and material), and nonelectrical (dielectric fluid and flow rate) parameters. Productivity and quality are directly related. Practically, the productivity increases with increasing the energy consumption (voltage, current, and pulse on time) and decreases with decreasing the energy consumption. On the other hand, surface finish would decrease with increasing the discharge voltage, current, and pulse width (Yeh et al., 2013; Yu et al., 2011).

In this research work, the authors would like to achieve higher productivity of the wire electrode in Wire-cut EDM associated with sustainable production in terms of work piece good surface quality and less heat-affected zone. Several efforts have been made to find the ideal machining conditions to enhance the productivity and improve the sustainability achieving high product quality by

* Corresponding author. Centre of Advanced Manufacturing and Material Processing, Department of Mechanical Engineering, Faculty of Engineering, University of Malaya, 50603 Kuala Lumpur, Malaysia. Tel.: +60 3 7967 4593; fax: +60 3 7967 5330.

E-mail address: ah_sarhan@yahoo.com (A.A.D. Sarhan).

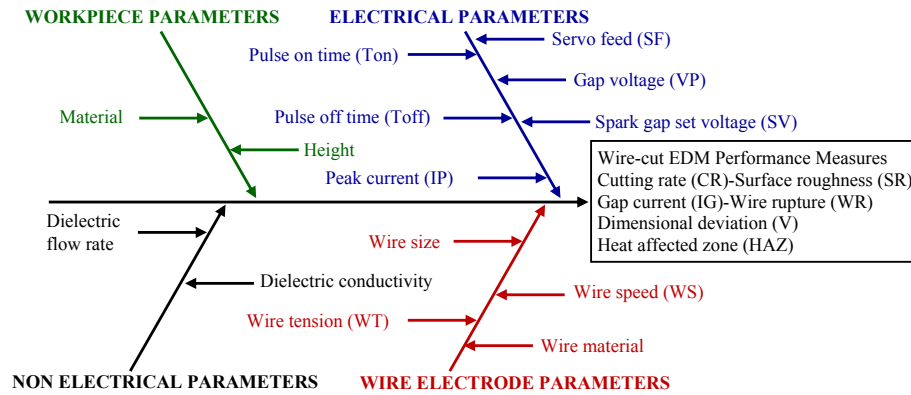


Fig. 1. W-EDM process parameters.

increasing the cutting rate and decreasing the surface roughness (Barzani et al., 2015; Kant and Sangwan, 2014). Nourbakhsh et al. (2013) studied the effect of injection pressure, servo reference voltage, time between two pulses and pulse width on surface integrity, wire rupture and cutting speed. It was revealed that cutting speed increases as pulse width increases; surface roughness decreases as the time between the two pulses decreases; and wire rupture is sensitive to injection pressure, wire mechanical tension, time between two pulses and pulse width. Besides, Gökler and Ozanözgü (2000) studied the effects of cutting parameters on the surface roughness of 1040, 2379 and 2738 steel and practical Wire cut-EDM results have been acquired. El-Hofy (2005) revealed that during Wire-cut EDM, the discharge temperature can reach up to 12,000 °C, and metallurgical changes happen in the workpiece surface layer. Moreover, a thin heat affected zone layer of 1 μm at 5 μj energy to 25 μm at high energy is formed. Levy and Maggi (1990) introduce that the heat-affected zone together with the solidified layer reaches 25 μm . The zone under the machined surface can be annealed. In addition, some of molten material is not ejected into the dielectric fluid and chills quickly, mainly by heat conduction into most of the workpiece, resulting in a hard surface. The annealed layer depth is proportional to the energy used in the cutting process. It is around 50 μm for finish cutting to approximately 200 μm for high cutting rates, as shown in Fig. 2 (El-Hofy, 2005; McGeough, 1988). The recast layer appears at different spark erosion conditions and it contains many pockmarks, globules, cracks, and micro cracks. There are three types of recast layers. Type 1 is a featureless, single layer less than 10 μm thick. Type 2 is an etchable, single layer 10–20 μm thick. Type 3 is a multilayer, 20 μm thick or greater, and consists of overlapping solidified layers (Tomlinson and Adkin, 1992). Researchers have carried out several investigations and have noted that this layer is obvious under all machining conditions, including when water is used as dielectric material (Jangra et al., 2011; Ramasawmy et al., 2005).

To acquire low surface roughness and small heat-affected zone, low discharge energy parameters (low energy consumption) with high dielectric flushing rate are required. However, such

parameters decrease the material removal rate. This implies that a high cutting rate with minimum surface defects is difficult to attain from a single parameter setting. To achieve the productivity of the wire electrode and good quality associated with sustainable production and low energy consumption; mathematical modeling between Wire-cut EDM parameters and performance measures should be obtainable to manufacturers. Theoretical and empirical approaches are commonly used for Wire-cut EDM modeling (Patil and Brahmanekar, 2010). Owing to the simplified and mandatory assumptions, the theoretical models yield big errors between the predicted and experimental results. Nevertheless, empirical models are limited to specific experimental conditions. The Taguchi method and response surface methodology (RSM) are the most often employed statistical techniques for determining the relationship between different controllable parameters and output performance (Davoodi and Tazehkandi, 2014; Hewidy et al., 2005). Moreover, Fuzzy logic and feed forward neural network has been used to model the process and correlate the parameters with the performance measures (Marani Barzani et al., 2015; Ooi et al., 2015). ANFIS has also been applied to model the process of predicting machining performance (Maher et al., 2015a, 2014). Although the optimization of process parameters have been considered in these techniques, there are limited studies about energy consumption of the wire-cut EDM, which are important for factor economics.

Because Wire-cut EDM involves multi-performance characteristics, the main objective of this study is to find a combination of Wire-cut EDM parameters to achieve rapid cutting speed as well as low surface roughness and small heat-affected zone to meet the demands for increasing the wire electrode productivity and product quality associated with sustainable production and low energy consumption. For this reason, ANFIS modeling is introduced as it is one of the soft computing techniques that play an important role in input–output parameter relationship modeling. Using ANFIS model, we can predict the required level of performance to increase the productivity at highest possible level of product quality for sustainable production.

2. Experimental work

In this research work, the experiments are carried out in wire-cut electric discharge machine to improve the productivity associated with better surface quality and minimum energy consumption for sustainable production. This section describes the experimental setup and the machined samples preparation for morphological characterization.



Fig. 2. EDM heat affected zone (El-Hofy, 2005).

2.1. Experimental setup

The experiments were performed using a computer numerical control (CNC) Sodick A500W Wire-cut EDM machine tool. Hard brass wire with 0.2 mm diameter, tensile strength of 1000 N/mm², elongation of 1.5% and electrical conductivity of 22% IACS was used for the machining blocks of AISI 1050 carbon steel under specific machining conditions.

The cutting speed was recorded directly from the Wire-cut EDM machine tool monitor. The surface roughness was measured with a stylus-based profilometer (Mitutoyo SJ-201, 99.6% accuracy). Scanning electron microscope (SEM) was used to examine the surface characteristics of the machined part and to measure the heat-affected zone thickness. The average cutting speed was calculated from the three, recorded data points under the same conditions. The average surface roughness was calculated for three different measurements under the same conditions with a sampling length of $L_c = 2.5$ mm at a specific workpiece area. The average heat-affected zone thickness was calculated from three measurements using image analysis software.

2.2. Machined samples preparation for morphological characterization

The raw material with 100 × 60 × 25 mm dimensions was machined into 5 × 5 × 25 mm for each specimen. The chemical compositions of AISI 1050 carbon steel was achieved by EDX machine as shown in Table 1. The electrical resistivity and thermal conductivity of AISI 1050 carbon steel were 1.63×10^{-5} Ω cm and 49.8 W/(m·K) respectively. Microscopic surface examinations after each grinding and finishing step were carried out using Olympus BX 61 light optical microscopy (OM). A scanning electron microscope (SEM) equipped with Energy-dispersive X-ray spectroscopy (EDS) (Hitachi tabletop microscope TM3030) was used to examine the surface microstructural and topographical characteristics and heat affected zone of the machined part.

3. Taguchi approach

Taguchi's parameter design is a powerful tool for determining near optimum design parameters for performance, quality, and cost. Orthogonal arrays, one of the major tools used in Taguchi design which study a large number of design variables with a small numbers of experiments. The second important tool used in Taguchi design is signal to noise (S/N) ratio, which used as a measurable values instead of standard deviations and mean. Taguchi introduces a two stage optimization technique, which produces a parameter level combination with minimum standard deviation while maintaining the mean on target (Su, 2013). Taguchi's approach is completely based on design of experiments (DOE), which optimize the process design and economically solving the problem. DOE is effective in studying the effects of many variables on performance as well as studying the influence of individual parameters to determine which variable has more influence on the performance measure (Roy, 2001).

The Taguchi full factorial design (L18) was selected with two machining variables with three levels and one machining variable with two levels, as shown in Table 2. The machining parameters,

Table 1
Chemical compositions of AISI 1050 carbon steel.

Element	C	Mn	P	S	Fe
Weight, Wt (%)	0.47–0.55	0.60–0.90	≤0.04	≤0.05	98.46–98.92

Table 2
Levels of machining parameters.

Machining parameter	Symbol	Units	Levels		
			Level 1	Level 2	Level 3
Pulse on time	Ton	μs	0.15	0.20	0.25
Wire tension	WT	g	300	350	400
Peak current	IP	A	16	17	–

including peak current (*IP*), pulse width (*Ton*) and wire tension (*WT*) were selected for this study to investigate the effect on machining performance, i.e., cutting speed (*CS*), surface roughness (*Ra*) and heat-affected zone (*HAZ*). The machining parameters and levels were selected based on previous experiments using one-factor-at-a-time approach. The other machining parameters were kept constant (Table 3) as recommended by the machine maker.

These parameter levels were selected within the limit range of a machine working with no wire breakage based on the initial investigation.

The goal of the experiment is to optimize the Wire-cut EDM variables to obtain high cutting speed values using the larger-is-better characteristic criteria (Equation (1)), and low surface roughness and heat-affected zone values using the smaller-is-better characteristic criteria (Equation (2)).

$$S/N = -10 \log\left(1/n \left(\sum (1/y^2)\right)\right) \quad (1)$$

$$S/N = -10 \log\left(1/n \left(\sum y^2\right)\right) \quad (2)$$

where n is the number of experiments, and y is the observed data.

Table 4 introduce the real data for cutting speed, surface roughness, and heat-affected zone. Table 5 shows signal to noise ratios of cutting speed, surface roughness, and heat affected zone. Tables 6–8 present the mean S/N ratios for each level of cutting speed, surface roughness, and heat-affected zone, respectively. These data were plotted as shown in Figs. 3–5, respectively. Figs. 3–5 indicate that peak current and pulse width are more significant to the mean S/N ratios for cutting speed, surface roughness, and heat-affected zone. Moreover, Figs. 3–5 depict that wire tension does not affect cutting speed or the heat-affected zone. In addition, wire tension is significant on the average S/N response for surface roughness.

4. ANFIS modeling

ANFIS is a neuro-fuzzy approach, in which a fuzzy inference system employed in the framework of an adaptive neural network. ANFIS can be used to build an input–output mapping based on fuzzy if-then rules as well as preset input–output data pairs for neural network. The membership function parameters were computed by the ANFIS modeling to track the known experimental input–output data (Jang et al., 1997; Zalnezhad et al., 2013).

Table 3
Constant machining parameters.

Machining parameter	Value
Pulse off time	2 μs
Spark gap set voltage	21 V
Flush Pressure	14 kgf/cm ²
Water resistivity meter	6×10^4 Ω cm
Wire speed	3 m/min
Cut length	21.6 mm
Main power supply voltage	265 V

Table 4
Experimental design using L18 orthogonal array and results.

No.	Input			Es (μj)	Output											
	IP (A)	Ton (μs)	WT (g)		CS (mm/min)				Ra (μm)				HAZ (μm)			
					1	2	3	Avg	1	2	3	Avg	1	2	3	Avg
1	16	0.15	300	50.4	0.64	0.59	0.55	0.59	2.50	2.44	2.45	2.46	10.39	10.18	10.12	10.23
2			350	50.4	0.60	0.57	0.58	0.58	2.41	2.37	2.43	2.40	9.42	9.53	9.12	9.36
3			400	50.4	0.64	0.62	0.62	0.63	2.40	2.38	2.30	2.36	9.78	10.01	9.87	9.89
4		0.20	300	67.2	0.67	0.69	0.64	0.67	2.59	2.61	2.58	2.59	17.08	16.98	16.11	16.72
5			350	67.2	0.72	0.69	0.66	0.69	2.50	2.56	2.47	2.51	17.22	16.22	16.92	16.79
6			400	67.2	0.71	0.66	0.70	0.69	2.42	2.48	2.40	2.43	17.32	17.63	17.71	17.55
7		0.25	300	84	0.85	0.85	0.81	0.84	2.88	2.79	2.87	2.85	19.44	19.44	19.44	19.44
8			350	84	0.83	0.87	0.79	0.83	2.77	2.80	2.79	2.79	19.44	18.77	19.44	19.22
9			400	84	0.85	0.87	0.84	0.85	2.72	2.72	2.72	2.72	19.23	19.44	19.65	19.44
10	17	0.15	300	53.55	0.83	0.85	0.79	0.82	2.49	2.52	2.54	2.52	14.68	12.02	13.35	13.35
11			350	53.55	0.81	0.76	0.79	0.79	2.45	2.55	2.44	2.48	12.43	12.79	12.76	12.66
12			400	53.55	0.77	0.80	0.81	0.79	2.47	2.43	2.45	2.45	12.68	12.05	13.35	12.69
13		0.20	300	71.4	0.95	0.91	0.92	0.93	2.64	2.61	2.72	2.66	18.91	18.11	19.18	18.73
14			350	71.7	0.98	0.96	0.93	0.96	2.56	2.62	2.60	2.59	19.44	18.77	19.26	19.16
15			400	71.4	1.01	0.95	0.97	0.98	2.59	2.49	2.53	2.54	19.11	18.11	20.08	19.10
16		0.25	300	89.25	1.11	1.07	1.12	1.10	2.94	2.91	2.86	2.90	22.75	20.32	19.44	20.84
17			350	89.25	1.11	1.15	1.09	1.12	2.88	2.79	2.87	2.85	22.04	24.04	18.82	21.63
18			400	89.25	1.14	1.14	1.12	1.13	2.73	2.79	2.75	2.76	21.01	21.43	22.84	21.76

ANFIS uses five network layers to perform the following fuzzy inference steps as shown in Fig. 6: (1) input parameters, (2) fuzzy set database layer, (2) fuzzy rule base construction, (4) decision-making, and (5) output defuzzification.

Layer 1: the output of this layer is the degree to which the given input satisfies the linguistic label associated to this node. Gaussian

Table 5
S/N ratios of machining performance measures.

No.	S/N ratios		
	CS	Ra	HAZ
1	-4.61	-7.82	-20.20
2	-4.70	-7.60	-19.43
3	-4.01	-7.46	-19.90
4	-3.53	-8.27	-24.46
5	-3.19	-7.99	-24.50
6	-3.19	-7.71	-24.89
7	-1.49	-9.10	-25.77
8	-1.67	-8.91	-25.68
9	-1.42	-8.69	-25.77
10	-1.78	-8.03	-22.51
11	-2.05	-7.89	-22.05
12	-2.07	-7.78	-22.07
13	-0.59	-8.50	-25.45
14	-0.33	-8.27	-25.65
15	-0.16	-8.10	-25.62
16	0.84	-9.25	-26.38
17	0.98	-9.10	-26.70
18	1.08	-8.82	-26.75

Table 6
Response table for S/N Ratios of cutting speed (Larger is better).

Level	IP	Ton	WT
1	-3.0905	-3.2035	-1.8605
2	-0.4519	-1.8299	-1.8247
3	-0.2803	-1.6284	-1.6284
Delta	2.6386	2.9232	0.2321
Rank	2	1	3

Table 7
Response table for S/N ratios of surface roughness (Smaller is better).

Level	IP	Ton	WT
1	-8.173	-7.764	-8.493
2	-8.414	-8.139	-8.294
3		-8.977	-8.093
Delta	0.241	1.214	0.399
Rank	3	1	2

membership functions are usually used to denote the linguistic terms because the relationship between the cutting parameters and machining performance in Wire-cut EDM is not linear, as shown in Fig. 7(a).

Table 8
Response table for S/N ratios of heat affected zone (Smaller is better).

Level	IP	Ton	WT
1	-23.40	-21.03	-24.13
2	-24.80	-25.10	-24.00
3		-26.18	-24.17
Delta	1.40	5.15	0.17
Rank	2	1	3

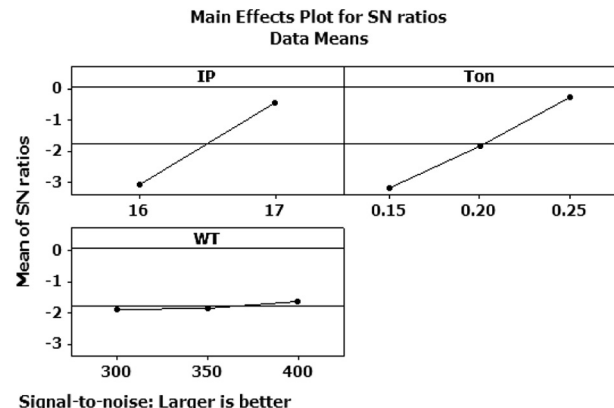


Fig. 3. Effect of process parameters on cutting speed.

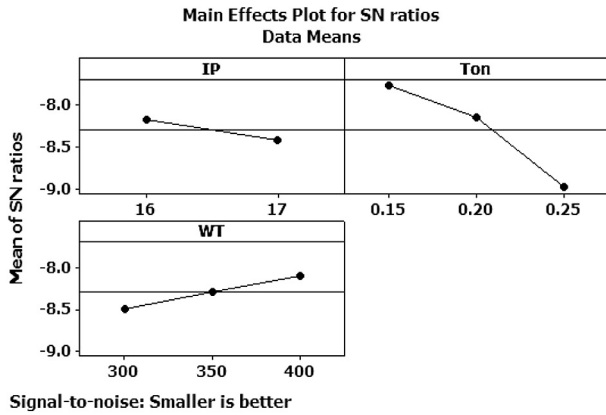


Fig. 4. Effect of process parameters on surface roughness.

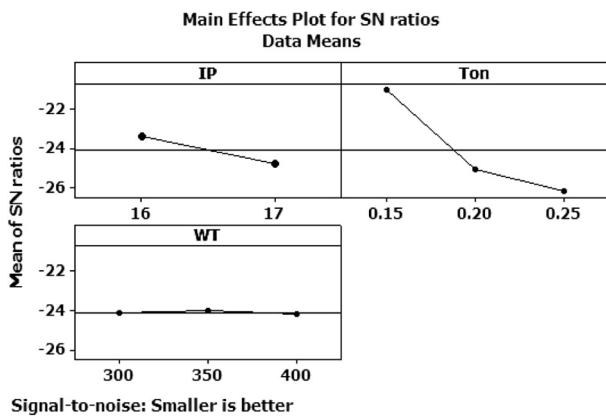


Fig. 5. Effect of process parameters on heat affected zone.

First parameter membership functions

$$A_i(IP) = \exp \left[-0.5 \left(\frac{IP - a_{i1}}{b_{i1}} \right)^2 \right] \quad (3)$$

Second parameter membership functions

$$B_i(Ton) = \exp \left[-0.5 \left(\frac{Ton - a_{i2}}{b_{i2}} \right)^2 \right] \quad (4)$$

Third parameter membership functions

$$C_i(WT) = \exp \left[-0.5 \left(\frac{WT - a_{i3}}{b_{i3}} \right)^2 \right] \quad (5)$$

where $a_{i1}, a_{i2}, a_{i3}, b_{i1}, b_{i2}, b_{i3}$ are the parameter set and $i = 1 - 2$ is for IP and $i = 1 - 3$ is for Ton and WT.

When the values of the parameter set change, the membership functions shape differ consequently (Fig. 7(b)), thus displaying several forms of membership functions on linguistic labels $A_i, B_i,$ and C_i . The parameters in this layer are referred to as principal parameters.

Layer 2: each neuron in this layer computes the firing strength of the associated rule. The output of each node is as follows:

$$\alpha_j = A_i(IP) \times B_i(Ton) \times C_i(WT) \quad (6)$$

Where $j = 1 - n, n$ is the number of rules.

Layer 3: each neuron in this layer computes the normalization of the firing levels. The output of each neuron is as follows:

$$\beta_j = \alpha_j / (\alpha_1 + \alpha_2 + \dots + \alpha_n) \quad (7)$$

Layer 4: each neuron in this layer computes the product of the normalized firing levels with the outputs of individual associated rule.

$$\beta_j F_j = \beta_j (a_{i1} + b_{i2} + c_{i3}) \quad (8)$$

Layer 5: the neuron in this layer computes the total system output as the sum of all incoming values.

$$CS, Ra, \text{ or } HAZ = \sum \beta_j F_j \quad (9)$$

If a crisp training set $((IP^k, Ton^k, WT^k) k = 1, \dots, K)$ is given, then the parameters of the neural net can be learned by descent type methods. The error function for pattern k is given by:

$$E_k = (z^k - o^k)^2 \quad (10)$$

where z^k is the wanted output and o^k is the calculated output by the neural network.

ANFIS was constructed in MATLAB, with 18 readings comprising the training data set listed in Table 4. Different membership functions were used to train ANFIS. Two membership functions of peak current and three membership functions of the other two parameters (pulse width and wire tension) were chosen to create the ANFIS model. The Gaussian membership function (gaussmf) gives

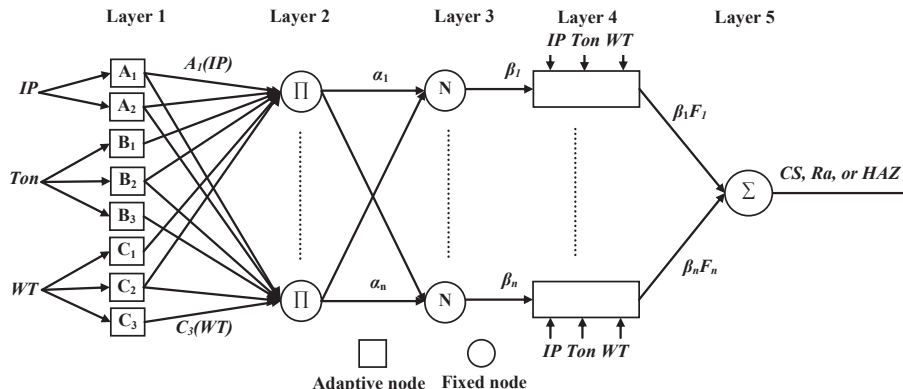


Fig. 6. ANFIS architecture for a three-input Sugeno fuzzy model.

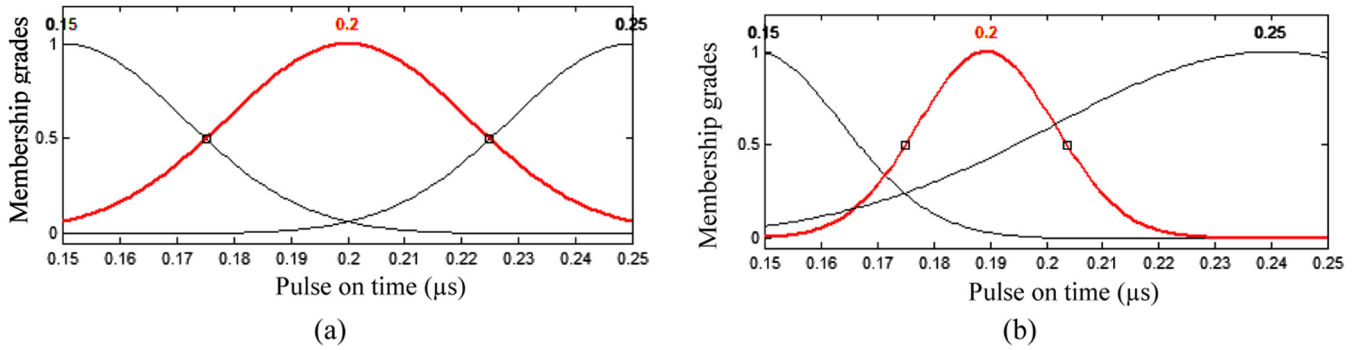


Fig. 7. Initial and final membership function of pulse on time (a) Initial membership function (b) Final membership function.

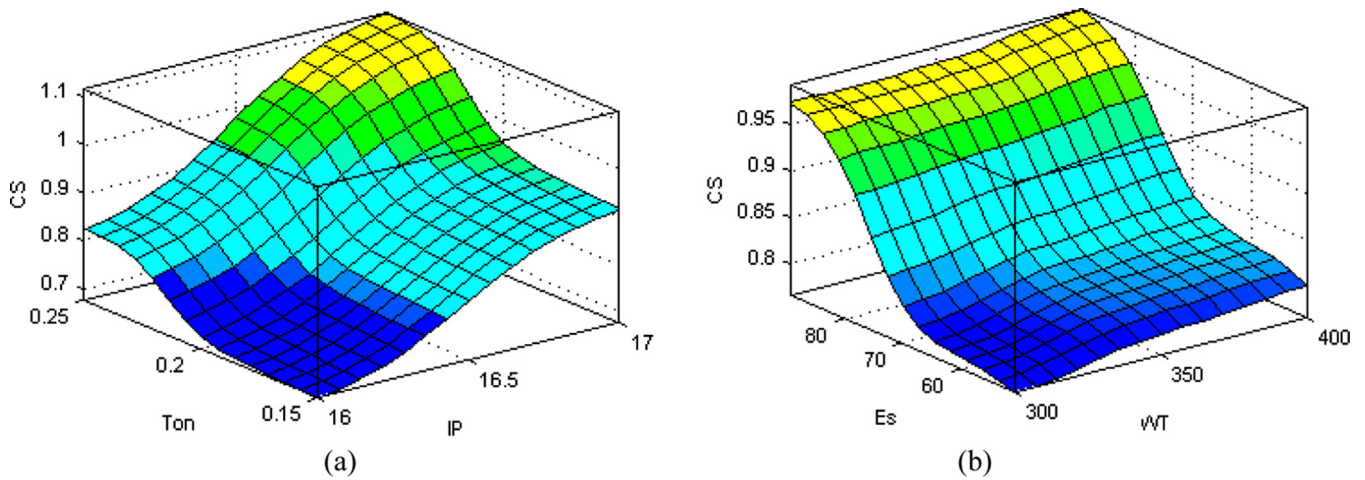


Fig. 8. The modeled cutting speed by ANFIS in relation to parameters change (a) Cutting speed in relation to change of pulse on time and peak current (b) Cutting speed in relation to change of wire tension and discharge energy.

the lowest training error of all performance measures, so it was adopted for the ANFIS training process in this study. The fuzzy rule architecture of ANFIS when gaussmf is adopted consists of 18 fuzzy rules generated from the input–output data set based on the Sugeno fuzzy model. During training, the 18 performance measure values (training data set) were used to conduct 50 cycles of learning

with an average error of 8.37×10^{-7} , 2.6×10^{-6} , and 1.5×10^{-5} for cutting speed, surface roughness, and heat-affected zone, respectively. Figs. 8–10 introduce the effects of the cutting parameters on the output performance based on the ANFIS models. Fig. 8–10 also show that the cutting speed, surface roughness, and heat-affected zone increase with increasing peak current and pulse width.

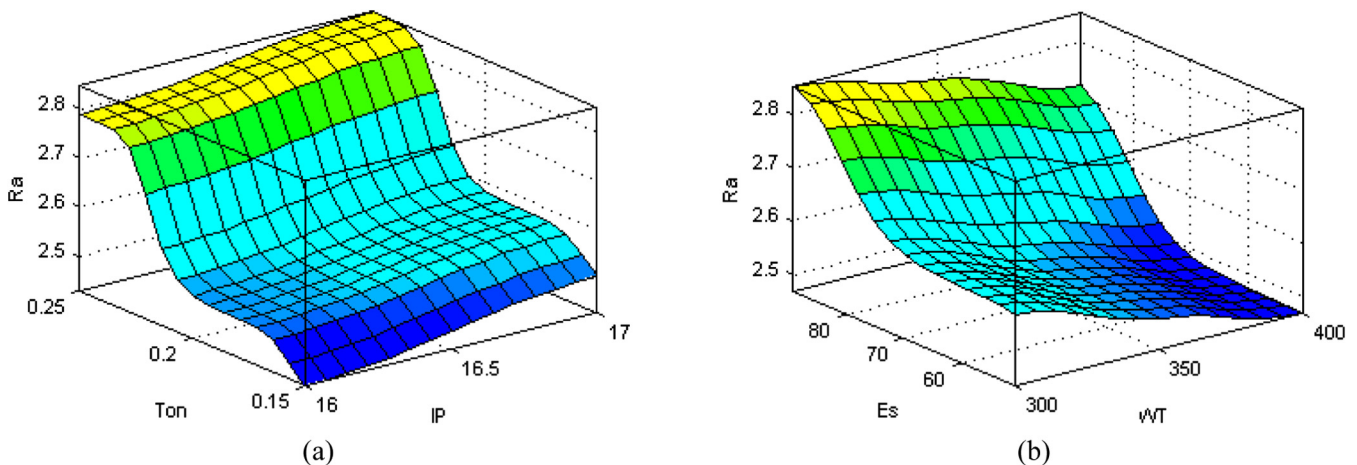


Fig. 9. The modeled Surface roughness by ANFIS in relation to parameters change (a) Surface roughness in relation to change of pulse on time and peak current (b) Surface roughness in relation to change of wire tension and discharge energy.

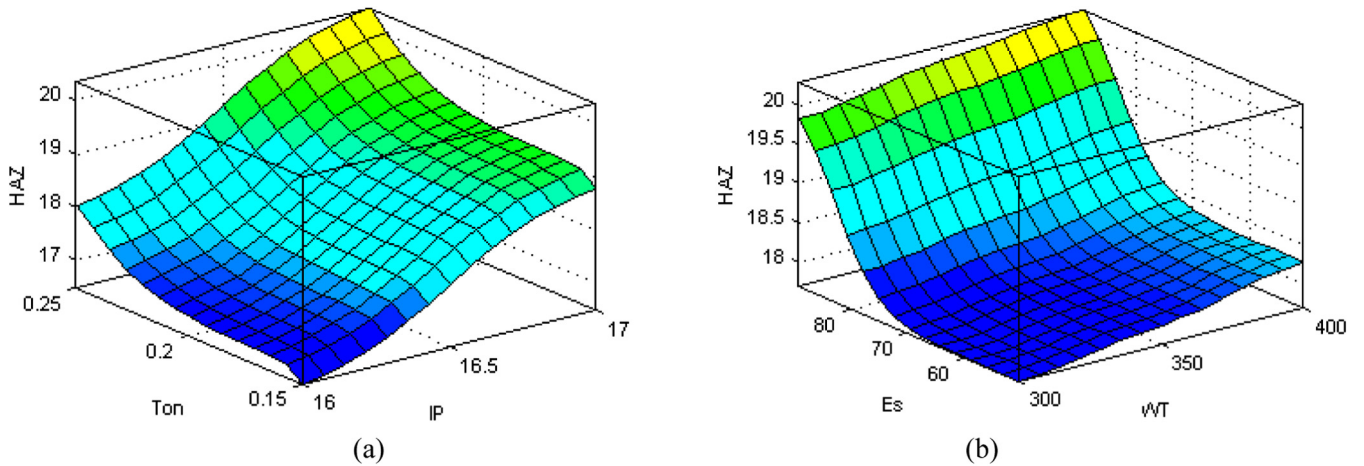


Fig. 10. The modeled Heat affected zone by ANFIS in relation to parameters change (a) Heat affected zone in relation to change of Pulse on time and peak current (b) Heat affected zone in relation to change of wire tension and discharge energy.

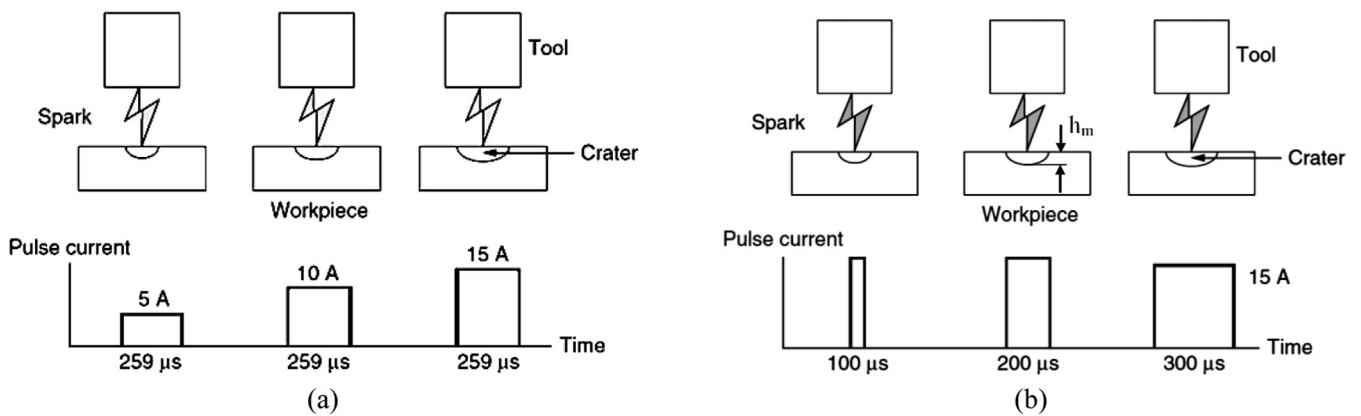


Fig. 11. Effect of spark energy on removal rate and surface roughness (a) Effect of pulse current on removal rate and surface roughness (b) Effect of pulse on time on removal rate and surface roughness.

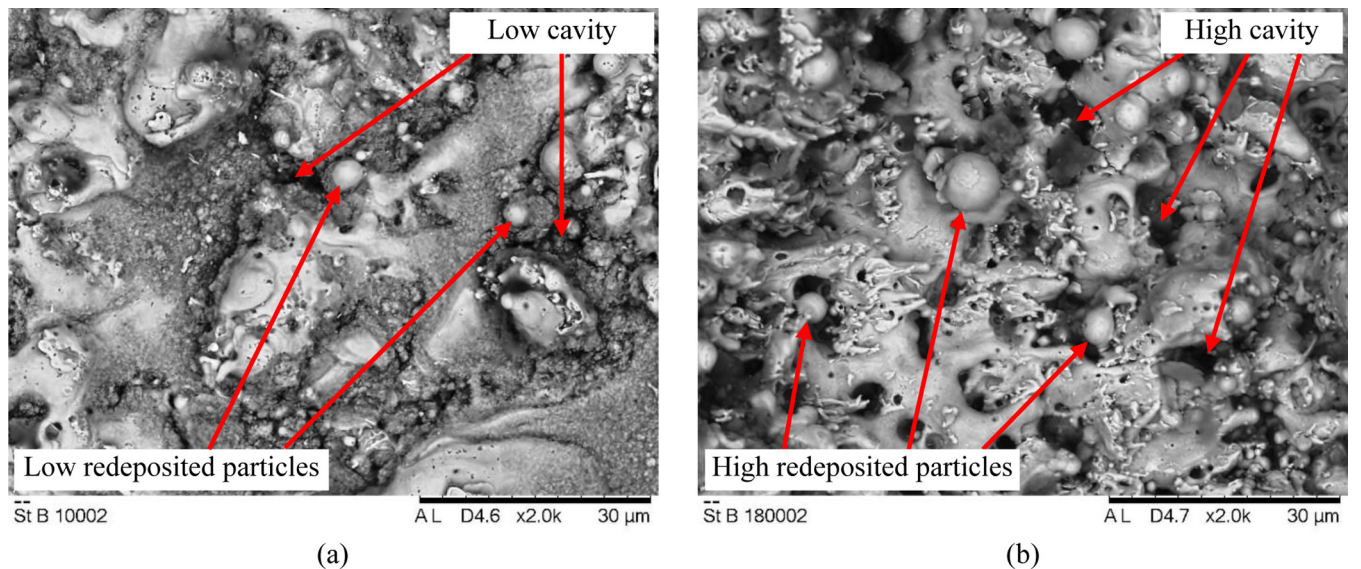


Fig. 12. SEM micrograph at different levels of spark energy (a) SEM micrograph at the lowest levels of peak current ($IP = 16\text{ A}$) and pulse on time ($Ton = 0.15\ \mu\text{s}$) (b) SEM micrograph at the highest levels of peak current ($IP = 17\text{ A}$) and pulse on time ($Ton = 0.25\ \mu\text{s}$).

Moreover, surface roughness decreases with increasing wire tension. Nevertheless, wire tension does affect the cutting speed and heat-affected zone.

5. Discussion

Fig. 3 suggests that peak current and pulse width are more significant for cutting speed. Wire tension is not significant on the average S/N ratio for cutting speed. The highest peak current and pulse width appear to be the best choice to obtain a high cutting speed value, thus making the process robust to peak current and pulse width in particular.

The same conclusions were drawn from Fig. 8(a) and (b) where pulse width and peak current had considerable effect on cutting speed, while an increase in both pulse width and/or peak current led to an increase in cutting speed, but wire tension had a minor effect on cutting speed, same end obtained by Maher et al. (2015b). Moreover, cutting speed (productivity) has major effect on energy consumption where the increase of cutting speed increases the energy consumption as shown in Fig 8(b). Increasing pulse width and peak current values is recommended for higher productivity. The ANFIS model shows that maximum cutting speed is achieved at the highest levels of peak current and pulse width (high level of energy consumption and process cost). That is because the combination of pulse width and peak current determines the spark energy as shown in equation (11) and hence the quantity of heat required to remove a definite volume of material. By increasing the pulse width and peak current, a large crater has to be cut per spark, as shown in Fig. 11(a) and (b) thus, the energy consumption is high. Consequently, this would increase the heat energy, leading to increased cutting speed as shown in equation (12) (El-Hofy, 2005).

$$Es = IP \times V \times Ton \quad (11)$$

$$CS \propto Es / (Ton + Toff) \quad (12)$$

Where V is the spark gap set voltage.

Fig. 4 indicates that pulse width and wire tension are more significant, followed by peak current on average S/N ratio for surface roughness. The lowest values of pulse width and peak current

and the highest value of wire tension are the best choices to attain a low surface roughness value.

In addition, Fig. 9(a) and (b) show that surface roughness increases as peak current, pulse width, and spark energy increase, but there are minor changes as wire tension increases. The SEM micrographs of the machined surface at 2000× magnification with the lowest and highest levels of peak current and pulse width are shown in Fig. 12(a) and (b) respectively. The SEM micrographs show that the cavity and redeposited particle with the highest levels of peak current and pulse width is higher than the lowest levels of peak current and pulse width. This is because the discharge energy increases with peak current and pulse width. Hence, larger craters are produced that lead to greater workpiece surface roughness (Kumar and Agarwal, 2012). This can be proved by the theory shown in Fig. 11(a) and (b) and equation (13) (El-Hofy, 2005).

$$hm \propto (Es)^{1/3} \quad (13)$$

A study of Fig. 5 suggests that pulse width and peak current are more significant, and wire tension is insignificant on the average S/N response of the heat-affected zone. The smallest values of peak current and pulse width appear to be the best choices to obtain a less thick heat-affected zone.

Based on the ANFIS model (Fig. 10(a), (b)), pulse width, and peak current has a great effect on the heat-affected zone but wire tension has a minor effect. The heat-affected zone width increases with increasing pulse width and/or peak current as shown in Fig. 10(a) and (b). Fig. 13(a) and (b) introduce SEM micrograph of the heat-affected zone. This micrograph verifies that the maximum width of the heat-affected zone is obtained at the highest levels of peak current and pulse width and the smallest heat-affected zone width is at the lowest values of pulse width and peak current. This is because the heat energy increases with peak current and pulse width. Hence, more heat is produced on the machined surface that leads to a larger heat-affected zone on the workpiece (Saha et al., 2008).

6. Conclusions

In the present case study, two data analysis techniques were used to achieve high productivity and best surface quality for

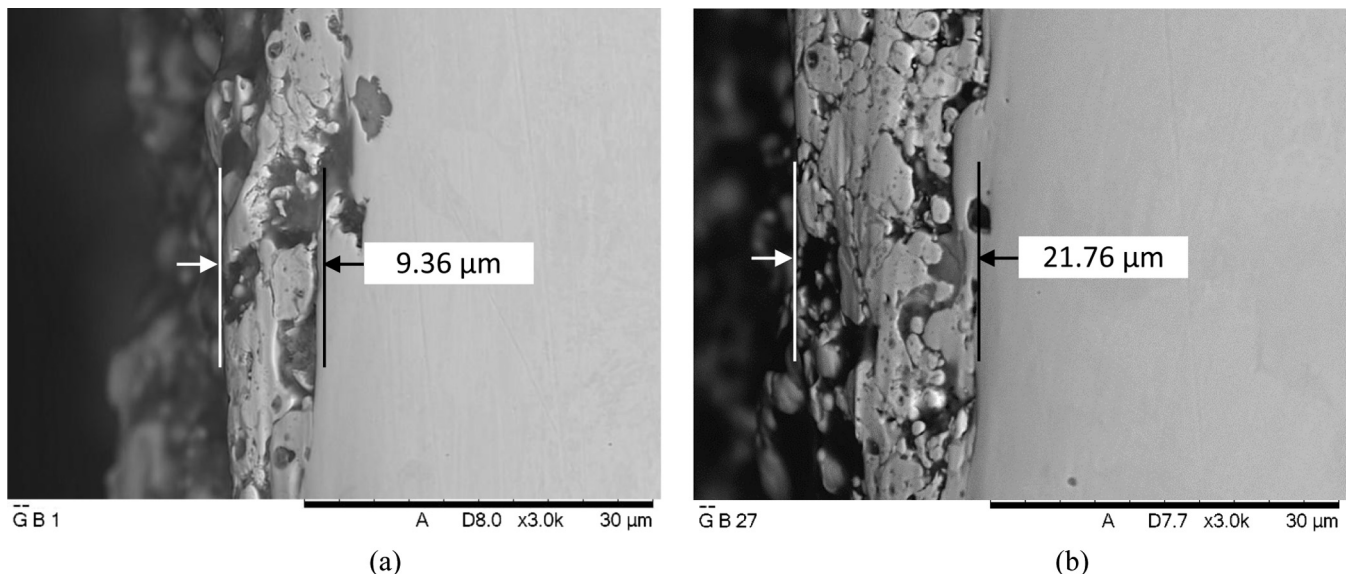


Fig. 13. Light optical microscope micrograph at different levels of spark energy (a) Light optical microscope micrograph for the lowest levels of peak current ($IP = 16$ A) and pulse on time ($Ton = 0.15 \mu s$) (b) Light optical microscope micrograph for the highest levels of peak current ($IP = 17$ A) and pulse on time ($Ton = 0.25 \mu s$).

sustainable production and low process cost in terms of product quality and less heat affected zone, from which similar conclusions were drawn. The peak current and pulse width (spark energy parameters) are the most significant parameters affecting cutting speed, surface roughness, and heat-affected zone. Wire tension has minor effect on cutting speed and heat-affected zone but it has pronounced effect on surface roughness. ANFIS was successfully used to develop an empirical model for modeling the relation between the predictor variables (Ton, IP, and WT) and the performance parameters (CS, Ra, and HAZ) to reduce the energy consumption and cost. The ANFIS models results are also compared with the Taguchi model results. As anticipated, the ANFIS models provide efficient prediction because they generally offer the ability to model more complex nonlinearities and interactions. In addition, by analyzing the results in Wire-cut EDM using the conceptual ANFIS approach, the following can be concluded:

1. ANFIS was used to introduce technological knowledge base for the selection of machining parameters to achieve high productivity at highest possible surface quality for sustainable production and lowering process cost.
2. High pulse width (0.25 μ s) and high peak current (17 A) are recommended to obtain high productivity for the definite test range.
3. Low pulse width (0.15 μ s), low peak current (16 A), and high wire tension (400 g) lead to smaller surface roughness values and heat affected zone for the specific test range.

Acknowledgments

This research was funded by the high impact research (HIR) grant number: HIR-MOHE-16001-00-D000027 from the Ministry of Higher Education, Malaysia, and the University of Malaya Post-graduate Research Grant (PPP) Program No. PG020-2013B.

References

- Barzani, M.M., Sarhan, A.A.D., Farahany, S., Ramesh, S., Maher, I., 2015. Investigating the machinability of Al–Si–Cu cast alloy containing bismuth and antimony using coated carbide insert. *Measurement* 62, 170–178. <http://dx.doi.org/10.1016/j.measurement.2014.10.030>.
- Davoodi, B., Tazehkandi, A.H., 2014. Experimental investigation and optimization of cutting parameters in dry and wet machining of aluminum alloy 5083 in order to remove cutting fluid. *J. Clean. Prod.* 68, 234–242. <http://dx.doi.org/10.1016/j.jclepro.2013.12.056>.
- El-Hofy, H., 2005. *Advanced Machining Processes*. McGraw-Hill Professional. <http://dx.doi.org/10.1036/0071453342>.
- Gökler, M.I., Ozanözgü, A.M., 2000. Experimental investigation of effects of cutting parameters on surface roughness in the WEDM process. *Int. J. Mach. Tools Manuf.* 40, 1831–1848. [http://dx.doi.org/10.1016/S0890-6955\(00\)00035-3](http://dx.doi.org/10.1016/S0890-6955(00)00035-3).
- Hewidy, M., El-Taweel, T., El-Safty, M., 2005. Modelling the machining parameters of wire electrical discharge machining of Inconel 601 using RSM. *J. Mater. Process. Technol.* 169, 328–336.
- Ho, K.H., Newman, S.T., Rahimifard, S., Allen, R.D., 2004. State of the art in wire electrical discharge machining (WEDM). *Int. J. Mach. Tools Manuf.* 44, 1247–1259. <http://dx.doi.org/10.1016/j.ijmachtools.2004.04.017>.
- Jang, J.-S.R., Sun, C.-T., Mizutani, E., 1997. *Neuro-fuzzy and Soft Computing: a Computational Approach to Learning and Machine Intelligence*. Prentice Hall, Inc, U.S.A.
- Jangra, K., Grover, S., Aggarwal, A., 2011. Simultaneous optimization of material removal rate and surface roughness for WEDM of WC-Co composite using grey relational analysis along with Taguchi method. *Int. J. Ind. Eng. Comput.* 2, 479–490. <http://dx.doi.org/10.5267/j.ijiec.2011.04.005>.
- Kant, G., Sangwan, K.S., 2014. Prediction and optimization of machining parameters for minimizing power consumption and surface roughness in machining. *J. Clean. Prod.* <http://dx.doi.org/10.1016/j.jclepro.2014.07.073>.
- Kumar, K., Agarwal, S., 2012. Multi-objective parametric optimization on machining with wire electric discharge machining. *Int. J. Adv. Manuf. Technol.* 62, 617–633. <http://dx.doi.org/10.1007/s00170-011-3833-1>.
- Levy, G.N., Maggi, F., 1990. WED machinability comparison of different steel grades. *CIRP Ann. Manuf. Technol.* 39, 183–185. [http://dx.doi.org/10.1016/S0007-8506\(07\)61031-2](http://dx.doi.org/10.1016/S0007-8506(07)61031-2).
- Maher, I., Eltaib, M.E.H., Sarhan, A.A.D., El-Zahry, R.M., 2015a. Cutting force-based adaptive neuro-fuzzy approach for accurate surface roughness prediction in end milling operation for intelligent machining. *Int. J. Adv. Manuf. Technol.* 76, 1459–1467. <http://dx.doi.org/10.1007/s00170-014-6379-1>.
- Maher, I., Eltaib, M.E.H., Sarhan, A.D., El-Zahry, R.M., 2014. Investigation of the effect of machining parameters on the surface quality of machined brass (60/40) in CNC end milling-ANFIS modeling. *Int. J. Adv. Manuf. Technol.* 74, 531–537. <http://dx.doi.org/10.1007/s00170-014-6016-z>.
- Maher, I., Ling, L.H., Sarhan, A.A.D., Hamdi, M., 2015b. Improve wire EDM performance at different machining parameters – ANFIS modeling. In: 8th Vienna International Conference on Mathematical Modelling (MATHMOOD 2015). IFAC, Vienna University of Technology, Vienna, Austria, pp. 105–110. <http://dx.doi.org/10.3182/20150218-3-AU-30250/978-3-902823-71-70082>.
- Maher, I., Sarhan, A.A.D., Hamdi, M., 2015c. Review of improvements in wire electrode properties for longer working time and utilization in wire EDM machining. *Int. J. Adv. Manuf. Technol.* 76, 329–351. <http://dx.doi.org/10.1007/s00170-014-6243-3>.
- Marani Barzani, M., Zalnezhad, E., Sarhan, A.A.D., Farahany, S., Ramesh, S., 2015. Fuzzy logic based model for predicting surface roughness of machined Al–Si–Cu–Fe die casting alloy using different additives-turning. *Measurement* 61, 150–161. <http://dx.doi.org/10.1016/j.measurement.2014.10.003>.
- McGeough, J.A., 1988. *Electrodischarge Machining, Advanced Methods of Machining*. Springer.
- Nourbakhsh, F., Rajurkar, K.P., Malshe, A.P., Cao, J., 2013. Wire electro-discharge machining of Titanium alloy. *Procedia CIRP* 5, 13–18. In: <http://dx.doi.org/10.1016/j.procir.2013.01.003>.
- Ooi, M.E., Sayuti, M., Sarhan, A.A.D., 2015. Fuzzy logic-based approach to investigate the novel uses of nano suspended lubrication in precise machining of aerospace AL tempered grade 6061. *J. Clean. Prod.* 89, 286–295. <http://dx.doi.org/10.1016/j.jclepro.2014.11.006>.
- Patil, N., Brahmankar, P.K., 2010. Determination of material removal rate in wire electro-discharge machining of metal matrix composites using dimensional analysis. *Int. J. Adv. Manuf. Technol.* 51, 599–610. <http://dx.doi.org/10.1007/s00170-010-2633-3>.
- Ramasawmy, H., Blunt, L., Rajurkar, K.P., 2005. Investigation of the relationship between the white layer thickness and 3D surface texture parameters in the die sinking EDM process. *Precis. Eng.* 29, 479–490. <http://dx.doi.org/10.1016/j.precisioneng.2005.02.001>.
- Roy, R.K., 2001. *Design of Experiments Using Taguchi Approach*. John Wiley & Sons, Inc.
- Saha, P., Singha, A., Pal, S., Saha, P., 2008. Soft computing models based prediction of cutting speed and surface roughness in wire electro-discharge machining of tungsten carbide cobalt composite. *Int. J. Adv. Manuf. Technol.* 39, 74–84. <http://dx.doi.org/10.1007/s00170-007-1200-z>.
- Sommer, C., Sommer, S., 2013. *Complete EDM Handbook*. Reliable EDM, Texas, USA.
- Su, C.-T., 2013. *Quality Engineering: Off-Line Methods and Applications*. CRC Press.
- Tomlinson, W.J., Adkin, J.R., 1992. Microstructure and properties of electrodischarge machined surfaces. *Surf. Eng.* 8, 283–288. <http://dx.doi.org/10.1179/sur.1992.8.4.283>.
- Yeh, C.-C., Wu, K.-L., Lee, J.-W., Yan, B.-H., 2013. Study on surface characteristics using phosphorous dielectric on wire electrical discharge machining of polycrystalline silicon. *Int. J. Adv. Manuf. Technol.* 69, 71–80. <http://dx.doi.org/10.1007/s00170-013-4995-9>.
- Yu, P.-H., Lin, Y.-X., Lee, H.-K., Mai, C.-C., Yan, B.-H., 2011. Improvement of wire electrical discharge machining efficiency in machining polycrystalline silicon with auxiliary-pulse voltage supply. *Int. J. Adv. Manuf. Technol.* 57, 991–1001. <http://dx.doi.org/10.1007/s00170-011-3350-2>.
- Zalnezhad, E., Sarhan, A.D., Hamdi, M., 2013. Investigating the effects of hard anodizing parameters on surface hardness of hard anodized aerospace AL7075-T6 alloy using fuzzy logic approach for fretting fatigue application. *Int. J. Adv. Manuf. Technol.* 68, 453–464. <http://dx.doi.org/10.1007/s00170-013-4743-1>.